The Journal of Immunology

Long-Acting Glucose-Dependent Insulinotropic Polypeptide Ameliorates Obesity-Induced Adipose Tissue Inflammation

Chen Varol, Isabel Zvibel, Lior Spektor, Fernanda Dana Mantelmacher, Milena Vugman, Tamar Thurm, Marian Khatib, Elinor Elmaliah, Zamir Halpern and Sigal Fishman

J Immunol 2014; 193:4002-4009; Prepublished online 12 September 2014;
doi: 10.4049/jimmunol.1401149
http://www.jimmunol.org/content/193/8/4002

The Journal of Immunology is published twice each month by
The American Association of Immunologists, Inc.,
1451 Rockville Pike, Suite 650, Rockville, MD 20852

Print ISSN: 0022-1767 Online ISSN: 1550-6606.

Long-Acting Glucose-Dependent Insulinotropic Polypeptide Ameliorates Obesity-Induced Adipose Tissue Inflammation

Chen Varol,*[,1] Isabel Zvibel,*[,1] Lior Spektor,* Fernanda Dana Mantelmacher,* Milena Vugman,* Tamar Thurm,* Marian Khatib,[†] Elinor Elmaliah,* Zamir Halpern,* and Sigal Fishman*

Obesity induces low-grade chronic inflammation, manifested by proinflammatory polarization of adipose tissue innate and adaptive resident and recruited immune cells that contribute to insulin resistance (IR). The glucose-dependent insulinotropic polypeptide (GIP) is an incretin hormone that mediates postprandial insulin secretion and has anabolic effects on the adipose tissue. Importantly, recent evidence suggested that GIP is a potential suppressor of inflammation in several metabolic models. In this study, we aimed to investigate the immunoregulatory role of GIP in a murine model of diet-induced obesity (DIO) using the long-acting GIP analog [*d*-Ala^2]GIP. Administration of [*d*-Ala^2]GIP resulted in adipocytes of increased size, increased levels of adipose tissue lipid droplet proteins, indicating better lipid storage capacity, and reduced adipose tissue inflammation. Flow cytometry analysis revealed reduced numbers of inflammatory Ly6C^{hi} monocytes and F4/80^{hi} CD11c$^+$ macrophages, associated with IR. In addition, [*d*-Ala^2]GIP reduced adipose tissue infiltration of IFN-γ–producing CD8$^+$ and CD4$^+$ T cells. Furthermore, [*d*-Ala^2]GIP treatment induced a favorable adipose tissue adipokine profile, manifested by a prominent reduction in key inflammatory cytokines (TNF-α, IL-1β, IFN-γ) and chemokines (CCL2, CCL8, and CCL5) and an increase in adiponectin. Notably, [*d*-Ala^2]GIP also reduced the numbers of circulating neutrophils and proinflammatory Ly6C^{hi} monocytes in mice fed regular chow or a high-fat diet. Finally, the beneficial immune-associated effects were accompanied by amelioration of IR and improved insulin signaling in liver and adipose tissue. Collectively, our results describe key beneficial immunoregulatory properties for GIP in DIO and reveal that its augmentation ameliorates adipose tissue inflammation and improves IR. ***The Journal of Immunology*****, 2014, 193: 4002–4009.**

During the last three decades, the prevalence of obesity has increased dramatically worldwide, leading to an explosion of health-related problems, including insulin resistance (IR), type 2 diabetes, coronary heart disease, and fatty liver (1). An increasing body of evidence points to a pivotal role for adipose tissue inflammation in the pathogenesis of obesity-related IR (2–5), and this association has become a target for new therapeutic modalities. The lipid storage capacity of adipocytes makes them gatekeepers for the levels of circulating free fatty acids. The inflammatory process starts with adipocyte apoptosis, which is induced when the maximal storage capacity of adipocytes has been reached, leading to recruitment of inflammatory cells and production of proinflammatory cytokines that induce local IR (2–5). Subsequently, adipose tissue IR leads to an increase in circulating free fatty acids that, in combination with proinflammatory cytokines, leads to systemic IR in skeletal muscle and liver (2–5).

Numerous studies have investigated the inflammatory process and immune cell populations in adipose tissue in diet-induced obesity (DIO) (2, 6–16). Adipose tissue macrophages (ATMs) are numerically and functionally different in lean and obese subjects. Accordingly, in lean mice, F4/80^{hi} resident ATMs constitute 10–15% of tissue cells, are characterized by an alternatively activated M2 phenotype, and enhance anabolic actions of insulin. In vast contrast, obesity and excess lipids classically activate the ATMs, polarizing them toward an M1 (inflammatory) state that is associated with secretion of inflammatory mediators, such as TNF-α, IL-6, and inducible NO synthase, which further contributes to the establishment of IR (2, 6–12). In particular, ablation of a specific proinflammatory ATM subset, characterized as F4/80^{hi}CD11b$^+$CD11c$^+$, reduces local and systemic proinflammatory cytokine levels and normalizes IR in DIO (11). Nevertheless, a recent study challenged the classical M1/M2 dogma, showing that obesity induces a program of lysosome biogenesis in ATMs and is coupled to lipid accumulation and catabolism but not a classic inflammatory M1 phenotype (17). The T cell compartment is also altered under obesity, resulting in a reduction in anti-inflammatory CD4$^+$Foxp3$^+$ regulatory T cells concomitant with augmentation of activated IFN-γ–producing effector CD4$^+$ and CD8$^+$ T cell populations responsible for aggravating adipose tissue inflammation (13–16).

Incretins, glucagon-like peptide 1 and glucose-dependent insulinotropic polypeptide (GIP), are hormones secreted from the small bowel in response to nutrients, and they act by increasing insulin secretion from the pancreas (18, 19). Both incretins are rapidly degraded and inactivated by dipeptidyl peptidase 4, a ubiquitous enzyme present on various cells (18, 19). Only glucagon-like peptide 1 analogs are used as therapeutic agents in type 2 diabetes, because, unlike GIP, they are insulinotrophic under hyperglycemic conditions.

*Research Center for Digestive Tract and Liver Diseases, Tel Aviv Sourasky Medical Center, Sackler Faculty of Medicine, Tel-Aviv University, Tel-Aviv 64239, Israel; and [†]Surgery Department, Tel-Aviv Sourasky Medical Center, Tel Aviv 64239, Israel

[1]C.V. and I.Z. contributed equally to this work.

Received for publication May 7, 2014. Accepted for publication August 6, 2014.

This work was supported by the Israeli Academy of Science (Grant 35/12 to S.F. and C.V.), the Israeli Society for the Study of Liver Disease (to S.F.), and Tel Aviv University (to S.F.).

Address correspondence and reprint requests to Dr. Sigal Fishman, Research Center for Digestive Tract and Liver Diseases, Tel Aviv Sourasky Medical Center, 6 Weizmann Street, Tel Aviv 64239, Israel. E-mail address: sigalf@tlvmc.gov.il

The online version of this article contains supplemental material.

Abbreviations used in this article: ATM, adipose tissue macrophage; BM, bone marrow; DIO, diet-induced obesity; GIP, glucose-dependent insulinotropic polypeptide; HFD, high-fat diet; IR, insulin resistance; ITT, insulin tolerance test; qRT-PCR, quantitative real-time RT-PCR; RC, regular chow; SVF, stromal vascular fraction; TG, triglyceride.

www.jimmunol.org/cgi/doi/10.4049/jimmunol.1401149

However, GIP may have other extrapancreatic beneficial effects. Specifically, in the adipose tissue, GIP potentiates the anabolic effects of insulin by increasing triglyceride (TG) uptake via lipoprotein lipase and, thus, increases lipid storage (20). In agreement with this, GIP inhibits adipose tissue lipolysis both in vitro and in vivo (21). In addition, GIP induces adipocyte maturation and differentiation (22).

The in vivo anti-inflammatory effect of GIP was suggested by studies showing reduced adipose tissue inflammatory cytokines in GIP-overexpressing transgenic mice (23) and by reduced atherosclerosis following administration of exogenous GIP (24, 25). Nevertheless, the role of GIP in adipose tissue inflammation with respect to mobilization and function of immune cells has not been thoroughly investigated. The present study investigated the in vivo effect of short-term or long-term administration of a long-lasting GIP analog, [*d*-Ala^2]GIP (26, 27), on the development of adipose tissue inflammation and immune cell recruitment in a murine DIO model. Our results show that administration of [*d*-Ala^2]GIP significantly reduced the levels of circulating proinflammatory neutrophils, as well as Ly6C^{hi} monocytes and their descendants, in the epididymal adipose tissue. Moreover, we report significant reduction in the accumulation of previously described proinflammatory CD11c$^+$ ATMs, together with reduced infiltration of IFNγ^+ CD8$^+$ and CD4$^+$ T cells. The beneficial anti-inflammatory effect of [*d*-Ala^2]GIP was further highlighted by the reduction in various inflammatory cytokines and chemokines and increased adiponectin expression. Finally, these immunological effects were accompanied by enhanced adipocyte storage capacity and improvement in metabolic parameters.

Materials and Methods

*Animals, DIO, and [*d*-Ala2]GIP administration*

C57BL/6 male mice (5 wk old, 19–21 g) were fed regular chow (RC) or a high-fat diet (HFD; 60% calories from fat; Research Diets, cat. no. D12492) for 10 wk (short regimen) or 14 wk (long regimen), and they received a single daily i.p. injection of human [*d*-Ala^2]GIP (0.12 μg/g body weight) (synthesized by Biosynthesis, Lewisville, TX) or vehicle (saline) during the last 2 wk (short regimen) or 8 wk (long regimen). Of note, previous studies used native human GIP and [*d*-Ala^2]GIP in rodent models (24–27). Animals had unrestricted access to food and water, were housed in temperature and humidity–controlled rooms, and were kept on a 12-h light/dark cycle. Thirty minutes before they were sacrificed, all mice received an i.p. injection of insulin (0.75 U/kg body weight). Blood was obtained from the left ventricle of the mice anesthetized with Pentol. Epididymal fat pads and livers were harvested and used for subsequent cell analysis, RNA extraction, and pathological assessments. All of the studies were approved by the Animal Care and Use Committee of the Tel-Aviv Sourasky Medical Center.

Ex vivo explants of human adipose tissue

Omental adipose tissue was obtained during sleeve gastrectomy from four obese patients (body mass index 35–40) who had signed consent forms (Helsinki approval 0397/11/TLV). The tissue was cut into small pieces (2–3 mm^3) and incubated for 2 h in DMEM (Life Technologies) supplemented with 10% FBS. The medium was removed and replaced with DMEM containing 0.5% BSA with 1 nM insulin and 100 nM [*d*-Ala^2]GIP for 24 h, and total RNA was extracted and used for quantitative real-time RT-PCR (qRT-PCR).

Insulin tolerance test

Two days before the end of the experiments, mice were subjected to 6 h of fasting, from 7:00 AM until 1:00 PM, and the basal glucose level was determined using the Accu-Chek Performa Sensor. Subsequently, insulin was administered by i.p. injection at a dose of 0.75 U/kg body weight, and serum glucose was measured at various time points thereafter.

Analytical procedures

Serum TGs and cholesterol were measured using a Hitachi 747 Automatic Analyzer. Serum adiponectin (Acrp30) was measured using a murine-specific ELISA kit (Millipore), according to the manufacturer's instructions.

Cell isolation procedure from adipose tissue and peripheral blood

The stromal vascular fraction (SVF) from murine adipose tissue was isolated as previously described (7). In brief, epididymal fat pads were surgically removed from mice, cut into small pieces, and incubated in digestion buffer (DMEM, 12.5 mM HEPES [pH 7.4], 2% BSA, and 10 mg collagenase type II [Sigma, St. Louis, MO]) for 20 min at 37°C in a shaking bath at 100 rpm. The digested tissue was filtered through a 250-μM nylon sieve and centrifuged at room temperature at 500 × *g* for 5 min. The pellet was washed, and erythrocytes were lysed with RBCs lysis solution. Peripheral blood mononuclear and polymorphonuclear cells were isolated using BD FACS Lysing Solution (Becton Dickinson, cat. no. 349202), according to the manufacturer's instructions.

Flow cytometry analysis and sorting of adipose tissue ATMs

Abs used for analysis of epididymal adipose tissue SVF-derived ATMs and T cell staining included previously used and calibrated Abs (28, 29): CD45.2 (104), Ly6C (HK1.4), CD11c (N418), CD11b (M1/70), I-Ab (AF6-120.1) (all from BioLegend), and F4/80 (CI:A3-1; Serotec) for ATMs and CD45.2 (104), CD3 (145-2C11), CD4 (GK1.5), IFN-γ (XMG1.2), IL-17A (TC11-18H10.1) (all from BioLegend), and CD8a (53.6.7; eBioscience) for T cells. Abs used for analysis of PBMCs included CD45.2 (104), CD115 (AFS98), Gr1 (Ly6G/C) (RB6-8C5), CD11b (M1/70), and CD3 (145-2C11) (all from BioLegend). All Ab staining for flow cytometry was performed following Fc blocking using the anti-mouse CD16/32 Ab (BioLegend; clone 93). Abs were used according to the manufacturer's instructions. For intracellular staining of IL-17A and IFN-γ in T cells, SVF cells were incubated for 4 h at 37°C with RPMI 1640 supplemented with 10% FCS, in the presence of 10 μg/ml brefeldin A, 10 ng/ml PMA, and 1 μg/ml ionomycin (Sigma). The cells were stained for surface markers of T cells, fixed and permeabilized, and then stained for the intracellular expression of IFN-γ and IL-17A. Cells were analyzed with a FACSCanto II or LSR Fortessa flow cytometer (Becton Dickinson) using FACS DIVA (Becton Dickinson) or FlowJo software.

Quantitative real-time RT-PCR

Total RNA was extracted from livers using the EZ-RNA kit (Biological Industries, Bet Haemek, Israel) and from adipose tissue using the RNeasy Lipid tissue kit (QIAGEN), and 200 ng–2 μg total RNA was reverse-transcribed using M-MLV (Promega, Madison, WI). qRT-PCR was performed using Absolute Blue qPCR SYBR Green ROX mix (Thermo Fisher Scientific, Epsom, Surrey, U.K.) in the Corbett rotor light cycler (Corbett Robotics, Brisbane, Australia). The murine and human intron span primers are listed in Supplemental Table I.

Protein immunoblots (Western blots)

Total protein from livers or adipose tissue was extracted by homogenization in ice-cold RIPA buffer (PBS, 1% Nonidet P-40, 0.5% sodium deoxycholate, 0.1% SDS, 1 mM PMSF, 5 μg/ml aprotinin, 10 μg/ml leupeptin, 1 μg/ml pepstatin A, and phosphatase inhibitors mixture). Homogenates were centrifuged for 25 min at 13,000 × *g*, supernatants were collected, and extracts were normalized to total protein content. Proteins were separated by SDS-PAGE and blotted onto nitrocellulose, and blots were blocked for 1 h in 5% milk. Blots were incubated overnight at 4°C with Abs to pAkt (Cell Signaling Technology, Danvers, MA; cat. no. 4060), Akt1/2 (Santa Cruz Biotechnology, Santa Cruz, CA), and GIPR (Santa Cruz Biotechnology; cat. no. sc-69417), incubated with HRP-conjugated secondary Ab, and subjected to chemiluminescent detection using the MicroChemi imaging system (DNR Bio-Imaging Systems). Densitometry was performed using ImageJ software, and expression of pAkt was normalized to expression of Akt.

Statistical analysis

The results are presented as mean ± SEM. Statistical significance was assessed using a two-tailed Student *t* test, with p values < 0.05 considered significant.

Results

*Treatment with [*d*-Ala^2]GIP enhances adipose tissue lipid storage capacity along with amelioration of inflammation*

To investigate the role of GIP in a metabolic model, we implemented the well-characterized murine DIO model of diet-induced IR. Our strategic experimental approach was based on augmentation of physiological GIP levels by injection of the long-lasting GIP agonist [*d*-Ala^2]GIP (26, 27) during the last 8 wk of a 14-wk HFD regimen. We started the HFD regimen in 5-wk-old mice, since animals of the same age were used in a previous study that thoroughly documented changes in ATMs and T cell populations from 2 to 20 wk HFD feeding compared with RC feeding (14).

We did not find any difference between mice fed HFD that received vehicle or [*d*-Ala^2]GIP with respect to food intake and total

Table I. Body parameters in mice after a 14-wk HFD or HFD with [*d*-Ala^2]GIP

	HFD	HFD + [*d*-Ala^2]GIP
Body weight (g)	38.2 ± 1.6	38.1 ± 0.7
Food intake (kcal/mouse/d)	11.4 ± 1.1	11.7 ± 1.2
Liver (g)	1.5 ± 0.1	1.2 ± 0.05*
Epididymal fat (g)	2.4 ± 0.1	2.5 ± 0.1
Total fat (g)	3 ± 0.1	3.3 ± 0.18
Percentage fat/body weight	7.9 ± 0.3	8.6 ± 0.4

Five-week-old C57BL/6 male mice received HFD for 14 wk; during the last 8 wk, they received daily i.p. injections of saline (n = 8) or [*d*-Ala^2]GIP (0.12 μg/g body weight) (n = 8).
*$p < 0.05$.

body and visceral fat weight (Table I). Obesity is characterized by fat hypertrophy and increased adipocyte area, accompanied by increased infiltration of immune cells into the visceral fat depots. Indeed, H&E staining of epididymal fat tissue sections from mice fed RC or HFD revealed dramatic immune cell infiltration and increased adipocyte area under DIO conditions (Fig. 1A). Strikingly, there was a >2-fold increase in the adipocyte area of mice receiving [*d*-Ala^2]GIP treatment, yet substantially reduced immune cell infiltration, in comparison with mice receiving HFD and vehicle (Fig. 1A, 1B). Previous studies established that GIP induces adipose tissue lipogenesis and TG uptake (20). Importantly, to our knowledge, we show for the first time the positive effect of [*d*-Ala^2]GIP treatment on the gene expression of lipid droplet proteins PLIN1, CIDEA, and CIDEC, as well as their transcription factor regulator, PPARγ (Fig. 1C). In particular, there was a 2-fold increase in the expression of CIDEA, which was positively associated with insulin sensitivity in obese human patients (30) (Fig. 1C). Similar effects on increased expression of genes for lipid droplet proteins also were observed after short-term [*d*-Ala^2]GIP treatment during the last 2 wk of the 10-wk HFD regimen (Supplemental Fig. 1C). Lastly, we determined the expression levels of GIPR within the adipose tissue after long-term treatment with [*d*-Ala^2]GIP and observed no significant change in [*d*-Ala^2]GIP–treated mice at either the mRNA (Fig. 1C) or protein (Supplemental Fig. 2) level, excluding the possibility of desensitization due to the [*d*-Ala^2]GIP treatment.

Treatment with [d-Ala^2]GIP reduces the numbers of proinflammatory adipose tissue macrophages, neutrophils, and T cell subsets

Several studies showed that obesity-induced inflammation is associated with infiltration of Ly6C^{hi} monocytes by virtue of their expression of the CCR2 chemokine receptor (9, 12). In line with the reduced immune cell infiltration seen in Fig. 1A, flow cytometry analysis revealed a significant 2-fold reduction in the recruitment and accumulation of monocytes characterized as Ly6C^{hi}CD11b^{hi}F4/80^{lo}CD11c^{-} in the adipose tissue of mice that received [*d*-Ala^2]GIP compared with mice that received vehicle only (Fig. 2A). Similarly, we also observed a clear reduction in resident ATMs, characterized as Ly6C^{lo}CD11b^{+} F4/80^{hi}CD11c^{-}, in the [*d*-Ala^2]GIP group (Fig. 2A). Notably, [*d*-Ala^2]GIP treatment resulted in a two-fold reduction in CD11c^{+}F4/80^{hi}CD11b^{+} ATMs (Fig. 2A), a population previously reported to play a deleterious proinflammatory role in obesity-induced IR (11).

Another inflammatory hallmark of DIO is the infiltration of both effector CD8^{+} and Th1 CD4^{+} T cells into the adipose tissue (13–15). Flow cytometry analysis at week 14 of the HFD regimen showed a significant reduction in the cell number of both CD8^{+} and CD4^{+} T cell populations in mice that received [*d*-Ala^2]GIP compared with mice that received vehicle only (Fig. 2B). Notably, T cell–derived IFN-γ was shown to induce adipocyte secretion of inflammatory chemokines and cytokines, and IFN-γ deficiency improved glucose tolerance in mice fed HFD (16). In this respect, we observed reduced numbers of IFN-γ–producing CD8^{+} and CD4^{+} T cells in mice treated with [*d*-Ala^2]GIP, with no effect on the numbers of Th17 T cells (Fig. 2B). With respect to neutrophils, GIP augmentation also resulted in their significantly reduced representation within the chronically inflamed epididymal adipose tissue (Fig. 2C).

Treatment with [d-Ala^2]GIP reduces the numbers of circulating monocytes and neutrophils in mice fed RC or HFD

We next examined the effect of long-term [*d*-Ala^2]GIP treatment on the composition of distinct immune cell entities in the circulation of

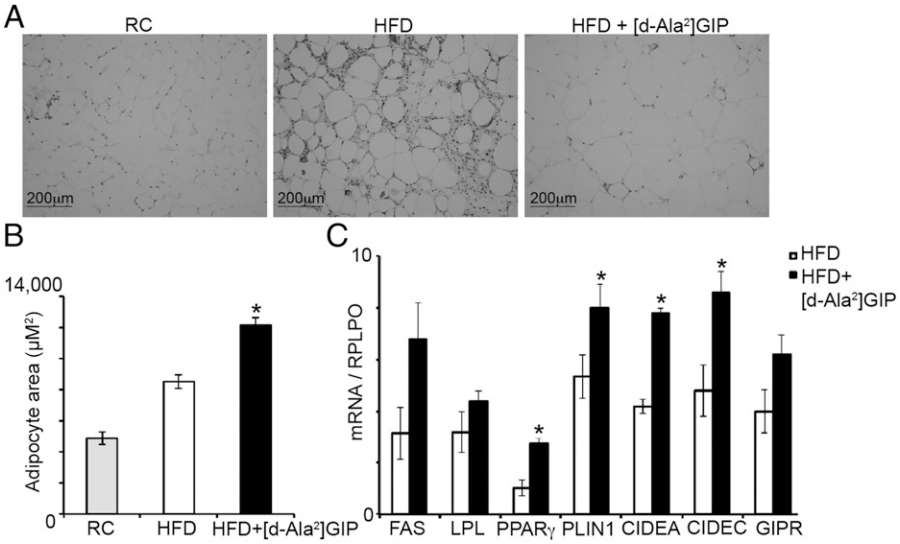

FIGURE 1. [*d*-Ala^2]GIP administration increases adipocyte storage capacity in DIO. (**A**) Representative H&E-stained paraffin sections of epididymal fat from mice fed RC, HFD for 14 wk and saline administration (HFD), or HFD for 14 wk with [*d*-Ala^2]GIP administration. Notice the impressive reduction in infiltration of immune cells and increase in adipocyte area in the [*d*-Ala^2]GIP–treated mice. (**B**) Adipocyte area calculated from epididymal fat of mice fed RC or HFD for 14 wk with vehicle or [*d*-Ala^2]GIP injections. Data are mean ± SEM. (**C**) Adipose tissue mRNA expression of metabolic enzymes, adipocyte markers of differentiation, and lipid droplet proteins from mice that received HFD or HFD with [*d*-Ala^2]GIP. Expression of the genes was detected by qRT-PCR and normalized to RPLPO. Data are mean ± SEM (n = 8/group). *$p < 0.05$.

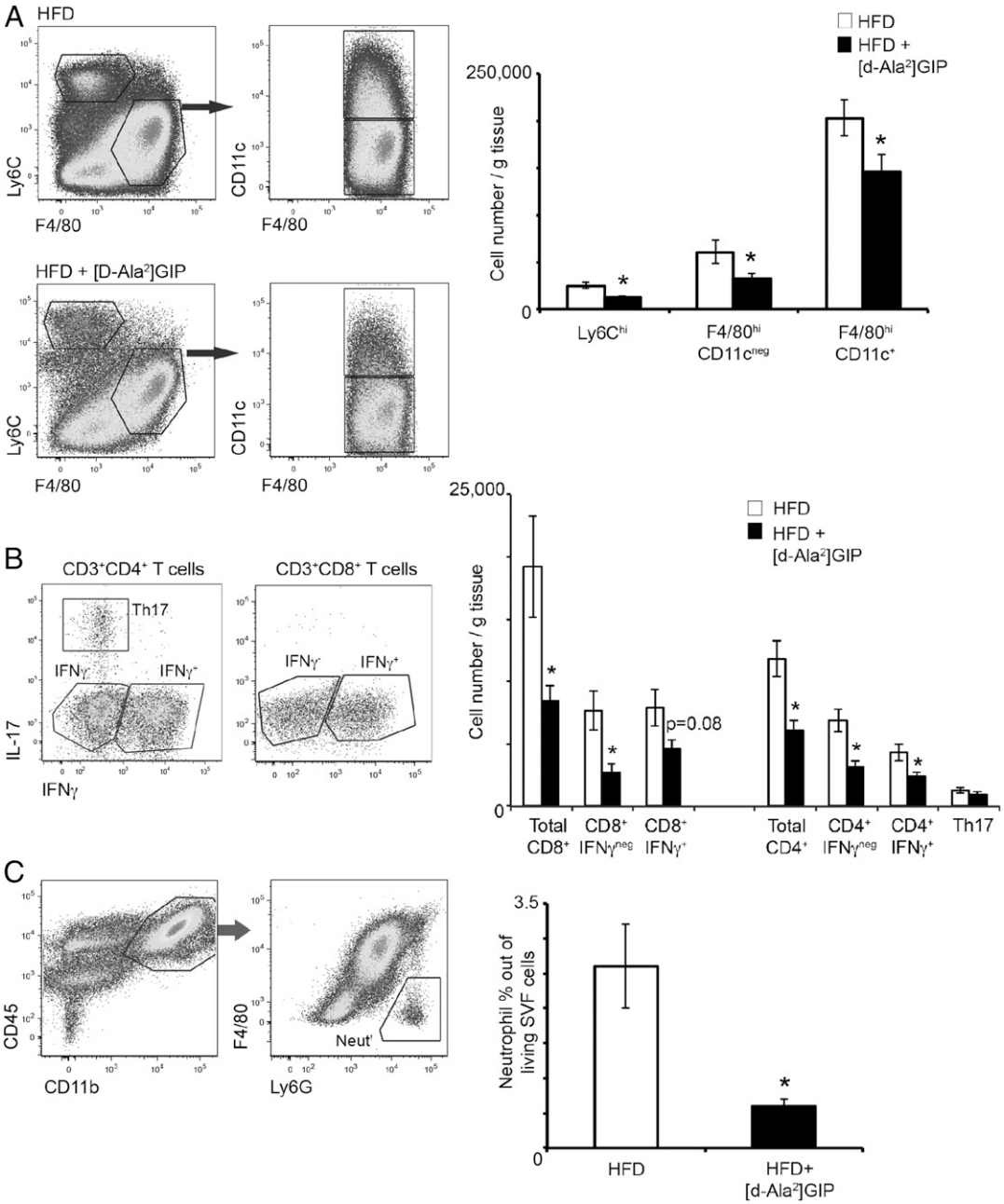

FIGURE 2. [*d*-Ala^2]GIP administration in a DIO model reduces the numbers of ATM subsets, CD4$^+$ and CD8$^+$ T cells, and neutrophils in epididymal fat. (**A**) Representative flow cytometry images showing the gating strategy used to define the distinct ATM subsets within the epididymal fat tissue of mice subjected to a 14-wk HFD regimen, with or without [*d*-Ala^2]GIP administration (*left panels*). Accordingly, gating on CD45$^+$ living cells, the monocyte-derived macrophages were characterized as Ly6C^{hi}CD11b^{hi}F4/80$^{-/lo}$CD11c$^-$, whereas resident ATMs were defined as F4/80^{hi}CD11b^{hi}Ly6C$^{-/lo}$CD11c$^-$. An additional proinflammatory ATM subset was characterized as F4/80^{hi}CD11b^{hi}Ly6C$^{-/lo}$CD11c$^+$ cells. ATM subset numbers (*right panel*). Data are mean ± SEM (n = 8/group), normalized per gram of tissue. (**B**) Representative flow cytometry images showing the gating strategy used to define CD8$^+$ and CD4$^+$ T cells expressing IFN-γ or IL-17 (*left panels*). Histogram showing numbers of epididymal fat tissue CD8$^+$ or CD4$^+$ T cells positive or negative for IFN-γ, as well as IL-17–producing Th17 T cells (*right panel*). Epididymal fat tissue was extracted from mice on 14 wk HFD treated with saline or [*d*-Ala^2]GIP. The graph shows mean ± SEM (n = 8/group), normalized per gram of tissue. (**C**) Representative flow cytometry image showing the gating strategy used to define neutrophils in the epididymal tissue (*left panels*). Epididymal fat neutrophil levels after a 14-wk HFD with saline or [*d*-Ala^2]GIP treatment (*right panel*). Data are mean ± SEM (n = 8/group). *$p < 0.05$.

mice on the 14-wk HFD. Flow cytometry analysis of peripheral blood demonstrated significantly reduced levels of circulating neutrophils characterized as Gr1(Ly6G/C)^{hi}CD115$^-$CD11b$^+$ (Fig. 3A). In addition, [*d*-Ala^2]GIP treatment reduced the numbers of both Ly6C^{hi} and Ly6C^{lo} CD115$^+$ blood monocyte subsets, but it had no effect on the levels of CD3$^+$ T cells (Fig. 3A). Moreover, short treatment (1 wk) with [*d*-Ala^2]GIP in mice fed RC also significantly reduced the numbers of circulating neutrophils (Fig. 3B), implying that[*d*-Ala^2]GIP regulates neutrophil egress from bone marrow (BM), irrespective of the metabolic state of the mice. In addition, BM flow cytometry analysis in the DIO model revealed increased numbers of neutrophils in the [*d*-Ala^2]GIP group, with no significant changes in Ly6C^{hi} monocytes or their precursors, macrophage dendritic cell precursor cells,

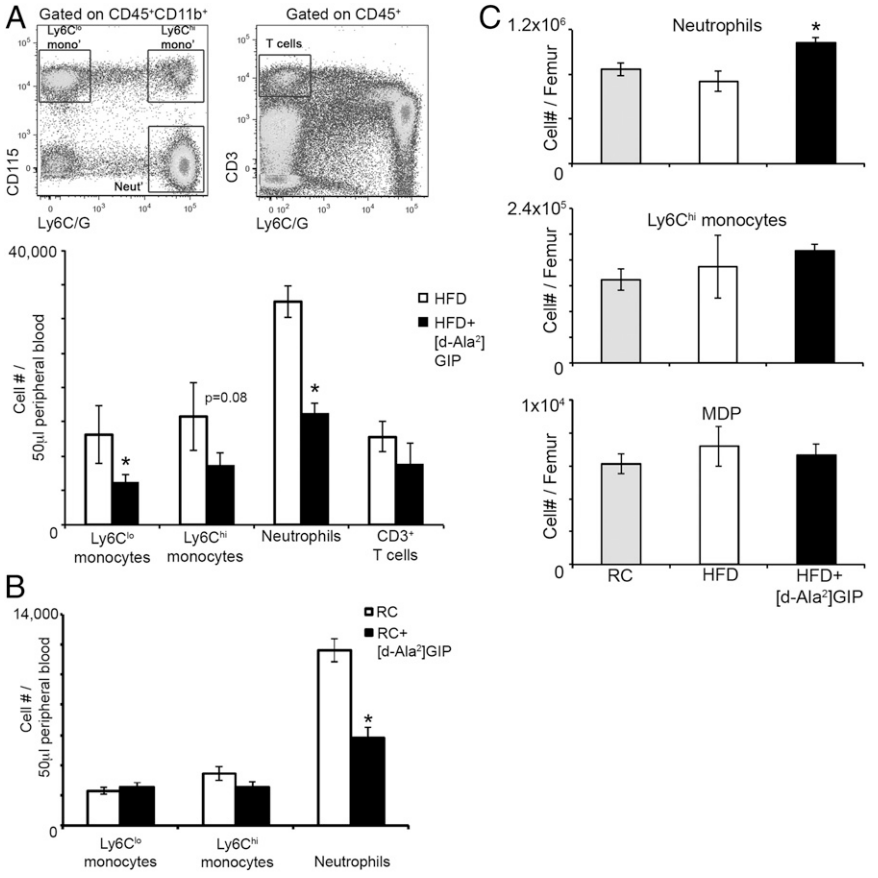

FIGURE 3. [*d*-Ala^2]GIP administration reduces the number of circulating BM-derived monocytes and neutrophils in mice after HFD and RC. (**A**) Representative flow cytometry images show the gating strategy used to define circulating immune cells in mice fed a 14-wk HFD (*upper panels*). Numbers of circulating T cells, neutrophils, and Ly6C^{hi} and Ly6C^{lo} monocytes collected from mice on a 14-wk HFD that were treated with saline or [*d*-Ala^2]GIP during the last 8 wk (*lower panel*). Data are mean ± SEM (n = 8/group), normalized per 50 µl of peripheral blood. (**B**) Numbers of peripheral blood immune cells collected from mice on RC that were treated with saline or [*d*-Ala^2]GIP for 7 d. Data are mean ± SEM (n = 8/group), normalized per 50 µl of peripheral blood. (**C**) Numbers of BM monocytes and neutrophils, as well as macrophage dendritic cell precursor cells (MDP), in mice fed RC or a 14-wk HFD and that received saline or [*d*-Ala^2]GIP treatment. *$p < 0.05$.

with the latter characterized as CD11b$^-$Gr1(Ly6C/G)$^-$cKit^{hi} CD115$^+$CD135$^+$ (Fig. 3C). Collectively, these results reveal that augmentation of GIP levels specifically reduces the numbers of proinflammatory circulating innate immune cells.

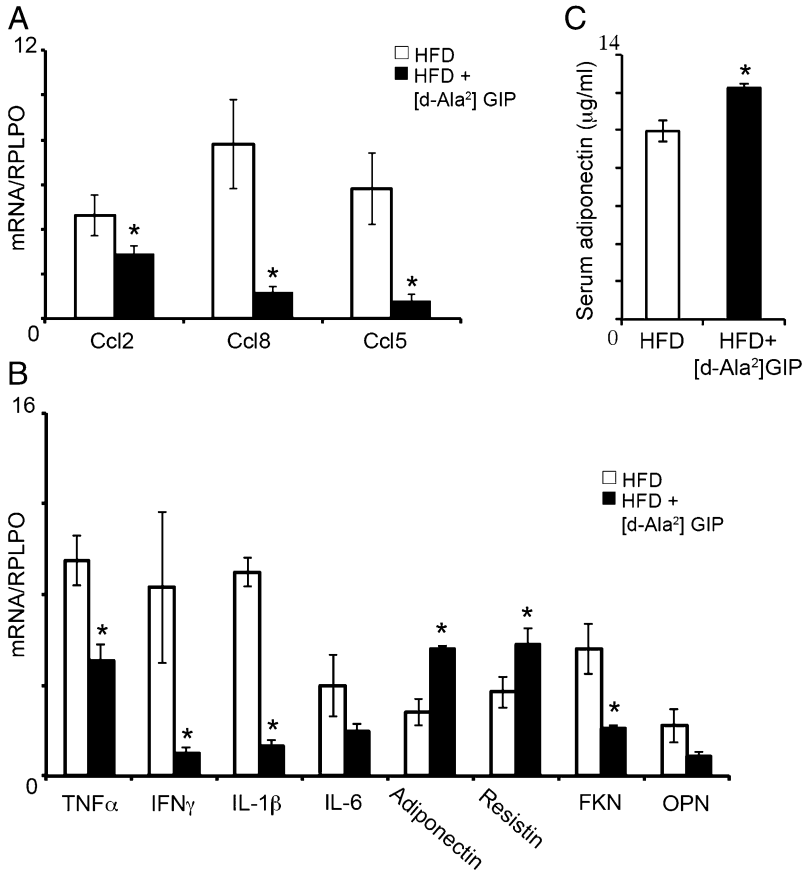

FIGURE 4. [*d*-Ala^2]GIP administration reduces adipose tissue inflammatory chemokines and cytokines in a DIO model. The mRNA expression of recruitment chemokines (**A**) and inflammatory cytokines (**B**) was assessed by qRT-PCR in epididymal fat of mice on a 14-wk HFD and treated with saline or [*d*-Ala^2]GIP. Data are mean ± SEM (n = 8/group). (**C**) Serum adiponectin levels in mice on a 14-wk HFD that received saline or [*d*-Ala^2]GIP. Data are mean ± SEM (n = 8/group). *$p < 0.05$.

Treatment with [d-Ala^2]GIP attenuates adipose tissue expression of inflammatory chemokines and cytokines in DIO

Monocyte recruitment from BM to the inflamed adipose tissue is mediated via CCR2 through binding to CCL5 or CCL8 chemokines, which are secreted by adipocytes or local immune cells (9, 12). In agreement with the reduction in Ly6C^{hi} monocytes in the adipose tissue (Fig. 2A), [*d*-Ala^2]GIP treatment significantly reduced the expression of CCL5 and CCL8 within the epididymal adipose tissue (Fig. 4A). In line with the observed reduction in T cell recruitment after [*d*-Ala^2]GIP treatment (Fig. 2B), we also saw a significant reduction in the T cell recruitment chemokine CCL5 (Fig. 4A). A similar reduction in the expression of recruitment chemokines was observed following short-term [*d*-Ala^2]GIP treatment (Supplemental Fig. 1A).

The inflammatory link between TNF-α and IL-1β and obesity-induced IR is well established (31–33). In this study, we showed, in a DIO model, that treatment with [*d*-Ala^2]GIP significantly ameliorated adipose tissue inflammation, manifested by a significant reduction in the expression of TNF-α and IL-1β after long (Fig. 4B) and short (Supplemental Fig. 1B) [*d*-Ala^2]GIP treatment. Osteopontin and fractalkine, both involved in the immune-regulation of IR, also were significantly lower in adipose tissue of [*d*-Ala^2]GIP mice (Fig. 4B). In accordance with reduced numbers of IFN-γ–producing T cells following [*d*-Ala^2]GIP treatment, there also was a significant reduction in adipose tissue mRNA levels of IFN-γ (Fig. 4B). Finally, we showed previously in rat and human ex vivo explants that [*d*-Ala^2]GIP administration significantly increased the expression of adiponectin, a well-known insulin-sensitizing adipokine (33). Strengthening these results, in this study we demonstrate in in vivo settings that GIP augmentation resulted in the profound increase of adipose tissue adiponectin mRNA in DIO after both long-term (Fig. 4B) and short-term [*d*-Ala^2]GIP administration (Supplemental Fig. 1B). The serum adiponectin levels also were increased by 20% in mice fed HFD that received [*d*-Ala^2]GIP (Fig. 4C). As expected, mRNA levels of resistin, a known target of GIP activation, also were elevated in the [*d*-Ala^2]GIP–treated group fed HFD (Fig. 4B).

[d-Ala^2]GIP treatment improves insulin sensitivity in DIO

The insulin tolerance test (ITT) assay revealed improved insulin sensitivity in mice on the HFD treated with [*d*-Ala^2]GIP compared with mice that received vehicle only, which was manifested by increased clearance of serum glucose (Fig. 5A). The increased insulin sensitivity following [*d*-Ala^2]GIP administration was corroborated by the significantly reduced area under the curve, calculated from the concentrations of glucose versus time (Fig. 5B). The improved insulin sensitivity induced by the long-term [*d*-Ala^2]GIP administration was further confirmed by the increased expression of the insulin-signaling key mediator pAkt, both in adipose tissue and in liver (Fig. 5C, 5D). However, although short-term [*d*-Ala^2]GIP treatment in DIO induced better glucose tolerance test, as exhibited by lower plasma glucose levels after high-dose IP glucose administration, it was not sufficient to improve insulin sensitivity, as determined by ITT (Supplemental Fig. 1D).

Ex vivo treatment of human obese patient–derived mesenteric adipose tissue with [d-Ala^2]GIP reduces expression of inflammatory cytokines

Adipose tissue explants obtained from obese patients were treated ex vivo with [*d*-Ala^2]GIP for 24 h and assessed for the expression of inflammatory cytokines and chemokines by qRT-PCR. We observed significant reductions in IL-6 and IL-1β and CCL8 mRNA, as well as a slight reduction in mRNA expression of CCL2 and CCL5, in the [*d*-Ala^2]GIP–treated explants (Fig. 6).

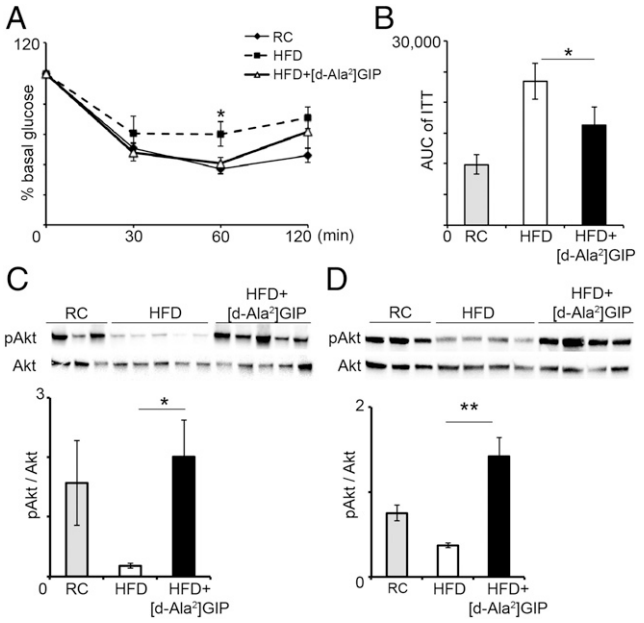

FIGURE 5. Treatment with [*d*-Ala^2]GIP leads to improved insulin sensitivity in a DIO model. (**A**) ITT of mice fed RC or a 14-wk HFD, with or without [*d*-Ala^2]GIP administration during the last 8 wk. Glucose concentration is expressed as the percentage of basal glucose levels (n = 5/group). (**B**) Area under the curve (AUC) calculated from the ITT curves of glucose concentrations versus time (n = 5/group). (**C**) Representative Western blot showing expression of pAkt in epididymal fat of mice fed a 14-wk HFD and injected with saline or with [*d*-Ala^2]GIP (*upper panel*). Expression of pAkt normalized to Akt (n = 5/group) (*lower panel*). (**D**) Representative Western blot showing expression of pAkt in livers of mice fed a 14-wk HFD and injected with saline or with [*d*-Ala^2]GIP (*upper panel*). Expression of pAkt normalized to Akt (n = 4/group). *$p < 0.05$, **$p < 0.01$.

Interestingly, progranulin, a newly described adipokine shown to be increased in serum of patients with IR (34), also was reduced by the [*d*-Ala^2]GIP treatment (Fig. 6).

Discussion

The present study investigated the effects of GIP at the interface between the metabolic and immunological arenas. We chose to focus on a 14-wk HFD regimen, a time period by which the mice are hyperglycemic and have developed profound IR and DIO-associated chronic inflammatory response involving both adaptive

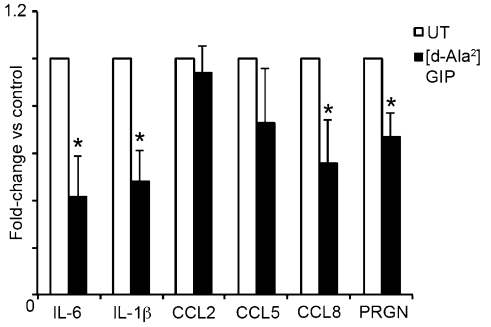

FIGURE 6. Ex vivo [*d*-Ala^2]GIP treatment reduces human adipose tissue inflammatory cytokines. Mesenteric adipose tissue from four obese patients was cultured as explants and treated with 1 nM insulin, with or without 100 nM [*d*-Ala^2]GIP, for 24 h. Expression of cytokines was determined by qRT-PCR and normalized to RPLPO. Data are mean fold-induction versus control for each explant (n = 4). *$p < 0.05$.

and innate immunity (14). The [*d*-Ala^2]GIP injections were initiated 6 wk after starting HFD, based on a previous study indicating this time as the beginning of the chronic inflammatory response (14). We show that GIP significantly reduced the accumulation of ATM subpopulations, as well as of adipose tissue IFN-γ–producing CD8$^+$ and CD4$^+$ T cells, which was accompanied by a significant reduction in various proinflammatory chemokines and cytokines. In addition, [*d*-Ala^2]GIP reduced the numbers of proinflammatory circulating monocytes and neutrophils. Importantly, all of these effects may explain the overall improved insulin sensitivity of the [*d*-Ala^2]GIP–treated mice. Our data suggest two possible mechanisms involved in GIP anti-inflammatory effects: reduced egress of monocytes and neutrophils from the BM or increased adipose tissue lipid storage capacity, resulting in reduced adipose tissue inflammation.

Adipose tissue from obese mice and humans is infiltrated with large numbers of macrophages, which play an initial dominant role in the development of systemic IR, glucose tolerance, and type 2 diabetes (6–12). In the current study, long-term treatment with [*d*-Ala^2]GIP significantly reduced the levels of three distinct ATM subsets: F4/80^{hi} CD11b^{hi}CD11c$^-$ resident ATMs, infiltrating Ly6C^{hi}CD11b^{hi} monocytes, and F4/80^{hi}CD11c$^+$ ATMs. Previous studies documented that the F4/80^{hi}CD11c$^+$ ATMs accumulate in adipose tissue during DIO by a CCR2-nondependent mechanism and express various inflammatory cytokines. Indeed, ablation of this population reversed HFD-induced IR (11). Furthermore, treatment with [*d*-Ala^2]GIP greatly reduced the adipose tissue infiltration by both CD8$^+$ and CD4$^+$ T cells and, specifically, IFN-γ–producing cells. Notably, obesity is associated with a reduction in anti-inflammatory Foxp3$^+$ regulatory T cells (13), in parallel with an increase in the accumulation of proinflammatory CD8$^+$ T cells and Th1 CD4$^+$ T cells in adipose tissue (14, 15). T cell–derived IFN-γ is a pivotal mediator of the obesity-induced chronic inflammatory response, and obese IFN-γ–deficient mice have significantly reduced adipose tissue expression of inflammatory mediators, such as TNF-α and CCL5, decreased inflammatory cell accumulation, and better glucose tolerance (16).

Continuous elevation of GIP levels in DIO reduced the levels of peripheral blood neutrophils and Ly6C^{hi} and Ly6C^{lo} monocytes. Of note, similar effects were obtained in mice on RC with short-term [*d*-Ala^2]GIP treatment, indicating that GIP may be involved with immune-regulatory pathways responsible for the development and migration of BM-derived neutrophils and monocytes, independently of the metabolic status of the organism. GIPR is present in the bone, both on osteoclasts and osteoblasts, and mediates GIP regulation of bone turnover, suggesting that GIP may act directly in the bone to prevent egress of immune cells (35). A second mechanism by which GIP may induce egress of immune cells from BM is via increased formation of corticosterone (36), a hormone that negatively regulates BM hematopoietic stem cells (37). Another possible mechanism through which GIP may interfere with the recruitment of CCR2$^+$ monocytes from the BM is via reduced adipose tissue expression of the CCR2 chemokines CCL5 and CCL8 (Fig. 4). Lastly, a recent article (38) described the inflammasome and IL-1β as the link between adipose tissue obesity-induced inflammation and myelopoiesis in the BM, compatible with our data showing reduced IL-1β in GIP-treated adipose tissue (Fig. 4).

In addition to the immune-regulatory effects of [*d*-Ala^2]GIP administration, we observed beneficial metabolic outcomes that may be attributed, in part, to the anti-inflammatory effects. To our knowledge, we show for the first time that GIP significantly increases the expression of the lipid droplet proteins CIDEA, CIDEC, and PLIN1 (Fig. 1). These proteins greatly enhance lipid droplet size, allowing greater adipose tissue lipid deposition and, thus, protecting other tissues from lipid accumulation (3). Indeed, the expression of lipid droplet proteins in adipose tissue of body mass index–matched obese humans positively correlates with insulin sensitivity (30). Thus, the GIP-governed increased lipid storage capacity of adipose tissue may reduce apoptosis and necrosis of adipocytes and attenuate the adipose tissue inflammatory cascade.

Finally, our results with human ex vivo explants strengthen the in vivo effects observed with [*d*-Ala^2]GIP in the DIO model and demonstrate direct anti-inflammatory effects of GIP on human adipose tissue. Especially interesting is the reduction of IR-associated progranulin, which was shown to be increased in adipose tissue following HFD and to enhance IR by increasing adipose tissue IL-6 expression (34). In conclusion, we demonstrated the effects of long-term GIP augmentation on circulating and adipose tissue innate and adaptive immune cells, culminating in an improved inflammatory and metabolic profile.

Acknowledgments

We thank M. Kaplan, DVM for excellent care of the animals.

Disclosures

The authors have no financial conflicts of interest.

References

1. Berrington de Gonzalez, A., P. Hartge, J. R. Cerhan, A. J. Flint, L. Hannan, R. J. MacInnis, S. C. Moore, G. S. Tobias, H. Anton-Culver, L. B. Freeman, et al. 2010. Body-mass index and mortality among 1.46 million white adults. *N. Engl. J. Med.* 363: 2211–2219.
2. Chawla, A., K. D. Nguyen, and Y. P. Goh. 2011. Macrophage-mediated inflammation in metabolic disease. *Nat. Rev. Immunol.* 11: 738–749.
3. Guilherme, A., J. V. Virbasius, V. Puri, and M. P. Czech. 2008. Adipocyte dysfunctions linking obesity to insulin resistance and type 2 diabetes. *Nat. Rev. Mol. Cell Biol.* 9: 367–377.
4. Osborn, O., and J. M. Olefsky. 2012. The cellular and signaling networks linking the immune system and metabolism in disease. *Nat. Med.* 18: 363–374.
5. Tilg, H., and A. R. Moschen. 2006. Adipocytokines: mediators linking adipose tissue, inflammation and immunity. *Nat. Rev. Immunol.* 6: 772–783.
6. Lumeng, C. N., J. L. Bodzin, and A. R. Saltiel. 2007. Obesity induces a phenotypic switch in adipose tissue macrophage polarization. *J. Clin. Invest.* 117: 175–184.
7. Lumeng, C. N., S. M. Deyoung, J. L. Bodzin, and A. R. Saltiel. 2007. Increased inflammatory properties of adipose tissue macrophages recruited during diet-induced obesity. *Diabetes* 56: 16–23.
8. Xu, H., G. T. Barnes, Q. Yang, G. Tan, D. Yang, C. J. Chou, J. Sole, A. Nichols, J. S. Ross, L. A. Tartaglia, and H. Chen. 2003. Chronic inflammation in fat plays a crucial role in the development of obesity-related insulin resistance. *J. Clin. Invest.* 112: 1821–1830.
9. Weisberg, S. P., D. Hunter, R. Huber, J. Lemieux, S. Slaymaker, K. Vaddi, I. Charo, R. L. Leibel, and A. W. Ferrante, Jr. 2006. CCR2 modulates inflammatory and metabolic effects of high-fat feeding. *J. Clin. Invest.* 116: 115–124.
10. Han, M. S., D. Y. Jung, C. Morel, S. A. Lakhani, J. K. Kim, R. A. Flavell, and R. J. Davis. 2013. JNK expression by macrophages promotes obesity-induced insulin resistance and inflammation. *Science* 339: 218–222.
11. Patsouris, D., P. P. Li, D. Thapar, J. Chapman, J. M. Olefsky, and J. G. Neels. 2008. Ablation of CD11c-positive cells normalizes insulin sensitivity in obese insulin resistant animals. *Cell Metab.* 8: 301–309.
12. Kamei, N., K. Tobe, R. Suzuki, M. Ohsugi, T. Watanabe, N. Kubota, N. Ohtsuka-Kowatari, K. Kumagai, K. Sakamoto, M. Kobayashi, et al. 2006. Overexpression of monocyte chemoattractant protein-1 in adipose tissues causes macrophage recruitment and insulin resistance. *J. Biol. Chem.* 281: 26602–26614.
13. Feuerer, M., L. Herrero, D. Cipolletta, A. Naaz, J. Wong, A. Nayer, J. Lee, A. B. Goldfine, C. Benoist, S. Shoelson, and D. Mathis. 2009. Lean, but not obese, fat is enriched for a unique population of regulatory T cells that affect metabolic parameters. *Nat. Med.* 15: 930–939.
14. Nishimura, S., I. Manabe, M. Nagasaki, K. Eto, H. Yamashita, M. Ohsugi, M. Otsu, K. Hara, K. Ueki, S. Sugiura, et al. 2009. CD8+ effector T cells contribute to macrophage recruitment and adipose tissue inflammation in obesity. *Nat. Med.* 15: 914–920.
15. Winer, S., Y. Chan, G. Paltser, D. Truong, H. Tsui, J. Bahrami, R. Dorfman, Y. Wang, J. Zielenski, F. Mastronardi, et al. 2009. Normalization of obesity-associated insulin resistance through immunotherapy. *Nat. Med.* 15: 921–929.
16. Rocha, V. Z., E. J. Folco, G. Sukhova, K. Shimizu, I. Gotsman, A. H. Vernon, and P. Libby. 2008. Interferon-gamma, a Th1 cytokine, regulates fat inflammation: a role for adaptive immunity in obesity. *Circ. Res.* 103: 467–476.

17. Xu, X., A. Grijalva, A. Skowronski, M. van Eijk, M. J. Serlie, and A. W. Ferrante, Jr. 2013. Obesity activates a program of lysosomal-dependent lipid metabolism in adipose tissue macrophages independently of classic activation. *Cell Metab.* 18: 816–830.
18. Baggio, L. L., and D. J. Drucker. 2007. Biology of incretins: GLP-1 and GIP. *Gastroenterology* 132: 2131–2157.
19. Paschetta, E., M. Hvalryg, and G. Musso. 2011. Glucose-dependent insulinotropic polypeptide: from pathophysiology to therapeutic opportunities in obesity-associated disorders. *Obes. Rev.* 12: 813–828.
20. Kim, S. J., C. Nian, and C. H. McIntosh. 2007. Activation of lipoprotein lipase by glucose-dependent insulinotropic polypeptide in adipocytes. A role for a protein kinase B, LKB1, and AMP-activated protein kinase cascade. *J. Biol. Chem.* 282: 8557–8567.
21. Gögebakan, Ö., J. Andres, K. Biedasek, K. Mai, P. Kühnen, H. Krude, F. Isken, N. Rudovich, M. A. Osterhoff, U. Kintscher, et al. 2012. Glucose-dependent insulinotropic polypeptide reduces fat-specific expression and activity of 11β-hydroxysteroid dehydrogenase type 1 and inhibits release of free fatty acids. *Diabetes* 61: 292–300.
22. Song, D. H., L. Getty-Kaushik, E. Tseng, J. Simon, B. E. Corkey, and M. M. Wolfe. 2007. Glucose-dependent insulinotropic polypeptide enhances adipocyte development and glucose uptake in part through Akt activation. *Gastroenterology* 133: 1796–1805.
23. Kim, S. J., C. Nian, S. Karunakaran, S. M. Clee, C. M. Isales, and C. H. McIntosh. 2012. GIP-overexpressing mice demonstrate reduced diet-induced obesity and steatosis, and improved glucose homeostasis. *PLoS ONE* 7: e40156.
24. Nogi, Y., M. Nagashima, M. Terasaki, K. Nohtomi, T. Watanabe, and T. Hirano. 2012. Glucose-dependent insulinotropic polypeptide prevents the progression of macrophage-driven atherosclerosis in diabetic apolipoprotein E-null mice. *PLoS ONE* 7: e35683.
25. Nagashima, M., T. Watanabe, M. Terasaki, M. Tomoyasu, K. Nohtomi, J. Kim-Kaneyama, A. Miyazaki, and T. Hirano. 2011. Native incretins prevent the development of atherosclerotic lesions in apolipoprotein E knockout mice. *Diabetologia* 54: 2649–2659.
26. Lamont, B. J., and D. J. Drucker. 2008. Differential antidiabetic efficacy of incretin agonists versus DPP-4 inhibition in high fat fed mice. *Diabetes* 57: 190–198.
27. Szalowska, E., K. Meijer, N. Kloosterhuis, F. Razaee, M. Priebe, and R. J. Vonk. 2011. Sub-chronic administration of stable GIP analog in mice decreases serum LPL activity and body weight. *Peptides* 32: 938–945.
28. Zigmond, E., S. Samia-Grinberg, M. Pasmanik-Chor, E. Brazowski, O. Shibolet, Z. Halpern, and C. Varol. 2014. Infiltrating monocyte-derived macrophages and resident kupffer cells display different ontogeny and functions in acute liver injury. *J. Immunol.* 193: 344–353.
29. Zigmond, E., C. Varol, J. Farache, E. Elmaliah, A. T. Satpathy, G. Friedlander, M. Mack, N. Shpigel, I. G. Boneca, K. M. Murphy, et al. 2012. Ly6C hi monocytes in the inflamed colon give rise to proinflammatory effector cells and migratory antigen-presenting cells. *Immunity* 37: 1076–1090.
30. Puri, V., S. Ranjit, S. Konda, S. M. Nicoloro, J. Straubhaar, A. Chawla, M. Chouinard, C. Lin, A. Burkart, S. Corvera, et al. 2008. Cidea is associated with lipid droplets and insulin sensitivity in humans. *Proc. Natl. Acad. Sci. USA* 105: 7833–7838.
31. Hotamisligil, G. S., N. S. Shargill, and B. M. Spiegelman. 1993. Adipose expression of tumor necrosis factor-alpha: direct role in obesity-linked insulin resistance. *Science* 259: 87–91.
32. Nov, O., A. Kohl, E. C. Lewis, N. Bashan, I. Dvir, S. Ben-Shlomo, S. Fishman, S. Wueest, D. Konrad, and A. Rudich. 2010. Interleukin-1beta may mediate insulin resistance in liver-derived cells in response to adipocyte inflammation. *Endocrinology* 151: 4247–4256.
33. Tilg, H., and G. S. Hotamisligil. 2006. Nonalcoholic fatty liver disease: Cytokine-adipokine interplay and regulation of insulin resistance. *Gastroenterology* 131: 934–945.
34. Matsubara, T., A. Mita, K. Minami, T. Hosooka, S. Kitazawa, K. Takahashi, Y. Tamori, N. Yokoi, M. Watanabe, E. Matsuo, et al. 2012. PGRN is a key adipokine mediating high fat diet-induced insulin resistance and obesity through IL-6 in adipose tissue. *Cell Metab.* 15: 38–50.
35. Yavropoulou, M. P., and J. G. Yovos. 2013. Incretins and bone: evolving concepts in nutrient-dependent regulation of bone turnover. *Hormones (Athens)* 12: 214–223.
36. Bates, H. E., J. E. Campbell, J. R. Ussher, L. L. Baggio, A. Maida, Y. Seino, and D. J. Drucker. 2012. Gipr is essential for adrenocortical steroidogenesis; however, corticosterone deficiency does not mediate the favorable metabolic phenotype of Gipr($^{-/-}$) mice. *Diabetes* 61: 40–48.
37. Kollet, O., Y. Vagima, G. D'Uva, K. Golan, J. Canaani, T. Itkin, S. Gur-Cohen, A. Kalinkovich, G. Caglio, C. Medaglia, et al. 2013. Physiologic corticosterone oscillations regulate murine hematopoietic stem/progenitor cell proliferation and CXCL12 expression by bone marrow stromal progenitors. *Leukemia* 27: 2006–2015.
38. Nagareddy, P. R., M. Kraakman, S. L. Masters, R. A. Stirzaker, D. J. Gorman, R. W. Grant, D. Dragoljevic, E. S. Hong, A. Abdel-Latif, S. S. Smyth, et al. 2014. Adipose tissue macrophages promote myelopoiesis and monocytosis in obesity. *Cell Metab.* 19: 821–835.